Bicyclo[3.2.1]amide-DNA: A Chiral, Nonchiroselective Base-Pairing System

Dae-Ro Ahn,[a] Anita Egger,[a] Christian Lehmann,[b] Stefan Pitsch,[c] and Christian J. Leumann*[a]

Abstract: The design, synthesis, and base-pairing properties of bicyclo[3.2.1]amide-DNA (bca-DNA), a novel phosphodiester-based DNA analogue, are reported. This analogue consists of a conformationally constrained backbone entity, which emulates a B-DNA geometry, to which the nucleobases were attached through an extended, acyclic amide linker. Homobasic adenine-containing bca decamers form duplexes with complementary oligonucleotides containing bca, DNA, RNA, and, surprisingly, also L-RNA backbones. UV and CD spectroscopic investigations revealed the duplexes with D- or L-complements to be of similar stability and enantiomorphic in structure. Bca oligonucleotides that contain all four bases form strictly antiparallel, left-handed complementary duplexes with themselves and with complementary DNA, but not with RNA. Base-mismatch discrimination is comparable to that of DNA, while the overall thermal stabilities of bca-oligonucleotide duplexes are inferior to those of DNA or RNA. A detailed molecular modeling study of left- and right-handed bca-DNA-containing duplexes showed only minor changes in the backbone structure and revealed a structural switch around the base-linker unit to be responsible for the generation of enantiomorphic duplex structures. The obtained data are discussed with respect to the structural and energetic role of the ribofuranose entities in DNA and RNA association.

Keywords: chirality · conformation analysis · DNA recognition · oligonucleotides · RNA

Introduction

Oligonucleotide analogues are of interest in antisense therapy and as tools in the area of functional genomics. In order to map the structure/stability landscape of oligonucleotides in complementary duplex formation, a number of DNA analogues have been synthesized and their base-pairing and antisense properties evaluated over recent years.[1] Major changes in the association behavior of oligonucleotides arise, as expected, from variation of the ribofuranose substructure in DNA and RNA. In this context, six-membered ring versions (e.g, homo-DNA,[2] HNA,[3] CeNA,[4] CNA,[5] p-RNA[6]) and four-membered ring versions (e.g, carbocyclic oxetanocine-DNA[7] and cyclobutane-DNA[8]), as well as ring-deficient analogues (such as *seco*-DNA[9, 10] and glycerol-DNA[11]) have been evaluated. Besides this, analogues of increased (seven bonds)[7] or decreased (five bonds)[12] length in the repetitive backbone unit have been evaluated.

In an effort to investigate various aspects of conformational restriction on the hybridization properties of DNA analogues,[13] we recently prepared and analyzed bicyclo[3.2.1]-DNA (Figure 1).[14–16] This analogue is composed of a rigid backbone unit of B-DNA geometry, to which the bases are flexibly attached through a methylenoxy linker unit. The main goal was to determine the impact on the duplexation properties of the loss of ring structure between base and backbone. We were able to show that bicyclo[3.2.1]-DNA is still a competent, but less effective, duplex partner for DNA, RNA,

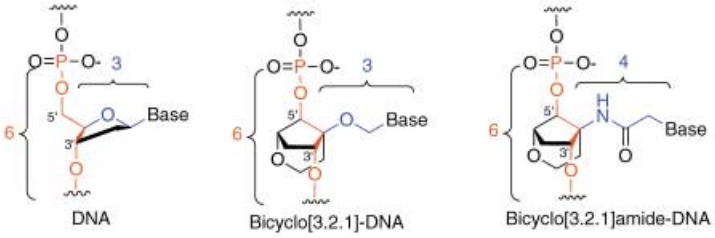

Figure 1. Chemical formulae of DNA, bicyclo[3.2.1]-DNA, and bicyclo[3.2.1]amide-DNA. The repetitive backbone bonds are highlighted in red, those of the base-linker elements in blue.

[a] Prof. C. J. Leumann, Dipl. Chem. D.-R. Ahn, Dipl. Chem. A. Egger
Department of Chemistry and Biochemistry
University of Bern
Freiestrasse 3, 3012 Bern (Switzerland)
Fax: (+41) 31-631-3422
E-mail: leumann@ioc.unibe.ch

[b] Dr. C. Lehmann
Institut de Chimie Organique
Université de Lausanne
Dorigny (Switzerland)

[c] Prof. S. Pitsch
Institut de Chimie Moléculaire et Biologique (ICMB)
EPFL, 1015 Lausanne (Switzerland)

0947-6539/02/0823-5312 $ 20.00+.50/0

and for itself. Furthermore, duplex formation is still orientation-specific (no parallel duplexes are formed), and base mismatches are discriminated equally well as in DNA. Thus, a number of necessary features for selective information transfer are still fulfilled in bicyclo[3.2.1]-DNA.

The basic framework of this bicyclo[3.2.1] scaffold offers a number of possible ways to change the molecular attachment of the nucleobases to the backbone. Thus, in analogy to the above-mentioned systems with elongated or shortened repetitive backbone units, we designed the bicyclo[3.2.1]amide-DNA (bca-DNA) as a DNA analogue in which the distance between the base and the backbone is elongated by one bond relative to DNA or bicyclo[3.2.1]-DNA, while the number of bonds in the repetitive backbone unit (six) remains unchanged. We report here on the synthesis, the base-pairing properties, and on structural investigations (by CD spectroscopy and molecular modeling) of bicyclo[3.2.1]amide-DNA in complexation with itself as well as with complementary DNA and RNA.

Results

Synthesis of monomers: We started the synthesis of the monomeric building blocks **5a–d** with the bicyclic backbone unit **1**, for which we had already developed a convenient access (Scheme 1).[17] Compound **1** was converted into compounds **3a–d** by amide bond formation with the nucleobase-bearing acetic acid derivatives **2a–d**, used previously for the synthesis of the polyamide nucleic acids (PNAs), and the uronium-based coupling reagent TOTU.[18–20] Despite the considerable steric hindrance of the amino group, acceptable to good yields were obtained. Compounds **3a–d** were subsequently tritylated to **4a–d** by treatment with dimethoxytrityl triflate (DMTOTf) in pyridine at slightly elevated temperatures. Desilylation with Bu_4NF in THF afforded **5a–d**, which could be phosphitylated with 2-cyanoethoxy diisopropylamino chlorophosphine (CEP) to give the building blocks for oligonucleotide synthesis **6a–d**, again in good yields. With these building blocks in hand we approached the automated oligonucleotide synthesis.

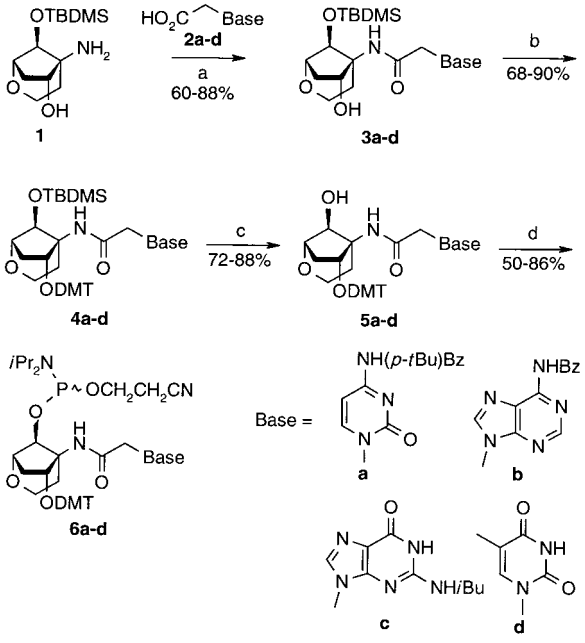

Scheme 1. Synthesis of the monomer building blocks **6**. a) *N*,*N*,*N*′,*N*′-tetramethyluronium tetrafluoroborate (TOTU), iPr_2NEt, DMF, room temperature; b) DMTOTf, pyr, 60 °C; c) Bu_4NF, THF, room temperature; d) iPr_2NEt, [(iPr_2N)($NCCH_2CH_2O$)]PCl, THF, room temperature.

Synthesis of oligonucleotides: Bicyclo[3.2.1]amide (bca) oligonucleotides **7–11** (Table 1) were prepared according to the standard protocols for automated DNA synthesis on the 1.3 μmol scale. Because of the reversed orientation of the dimethoxytrityl (O(3′)) and phosphityl (O(5′)) groups in the phosphoramidites **6a–d** relative to the deoxyribonucleoside phosphoramidites, synthesis of the bca-oligonucleotides proceeded in the 5′ → 3′ direction. As solid support, commercial thymidine-derived CPG was used for the synthesis of **10** and **11**, and a universal CPG solid support for oligonucleotides **7–9**. While the use of the former results in the attachment of a natural DNA unit at the 5′-end of the bca oligonucleotides, through a 5′–5′ junction, the advantage of the universal solid support lies in its traceless removal after synthesis and deprotection.

Table 1. Yield after HPLC purification (1.3 μmol scale), as well as sequence and MS data, of bca-oligonucleotides used in this study.

	Sequence (5′ → 3′)	$[M-H]^-$ (calcd)	ESI-MS (found)	Yield OD^{260} [%]
7	bca(GAGACCCGT)	3471.5	3471.2	12.6 (10)
8	bca(ACGGGTCTC)	3462.5	3462.0	16.6 (13)
9	bca(CTCTGGGCA)	3462.5	3462.0	24.4 (20)
10	bca(XA_{10})[a]	4205.2	4203.1[b]	42.3 (41)
11	bca(XT_{10})[a]	4115.1	4118.2[b]	37.4 (41)

[a] X = dT, arising from solid support. [b] MALDI-ToF MS.

The standard DNA synthesis cycle needed some adjustments. For complete removal of the dimethoxytrityl groups, 10% trichloroacetic acid in dichloroethane had to be used. Furthermore, the coupling time was extended to 6–10 min, and the standard activator tetrazole was replaced by the more active (*S*-benzylthio)-1*H*-tetrazole. With these changes, coupling yields of 94–99% were obtained, according to trityl assay. Crude oligonucleotides were deprotected and detached from the solid support in ammonia. Standard conditions (conc. NH_3, 55 °C, 16 h) were sufficient to release and deprotect the bca oligonucleotides prepared on dT solid support. No products arising from cleavage of the amide bond between base and backbone units were detected. Removal of the universal solid support, however, needed harsher conditions (NH_3, 70 °C, 48 h) and resulted in partial cleavage of (statistically) one base-linker unit (ESI-MS). These "abasic" oligonucleotides could, however, easily be removed by HPLC. All bca oligonucleotides were characterized by ESI mass spectrometry. We examined the structural and thermodynamic properties of duplex formation of bca oligonucleotides **7–11** with themselves and with the backbone systems of DNA, RNA, and L-RNA by CD spectroscopy and UV melting curve analysis.

  0947-6539/02/0823-5313 $ 20.00+.50/0

Pairing properties within the homobackbone series: Table 2 summarizes the thermal melting temperatures (T_m) as well as the thermodynamic data for duplex to single-strand transitions as determined by the concentration variation method.[21] Representative melting curves of the nonamer duplexes are depicted in Figure 2.

Table 2. T_m and thermodynamic data of duplex formation in the pure bca series.[a]

Entry		T_m[b]	ΔH [kJ mol^{-1}]	ΔS [J K^{-1} mol^{-1}]	ΔG^{298K} [kJ mol^{-1}]
1	bca(GAGACCCGT) (CTCTGGGCA)bca	31.7	−281.1	−809.7	−39.7
2	bca(GAGACCCGT) bca(CTCTGGGCA)	nd	–	–	–
3	bca(XA_{10}) bca(XT_{10})	21.6	−300.6	−911.5	−28.9
4	d(GAGACCCGT) (CTCTGGGCA)d	48.5	−280.1	−756.0	−54.6
5	d(A_{10}) d(T_{10})	32.4	−291.6	−849.3	−38.5

[a] Buffer conditions: 10 mM Na cacodylate, 1 M NaCl, pH = 7.0, total oligonucleotide concentration = 5 μM. [b] nd = not detected.

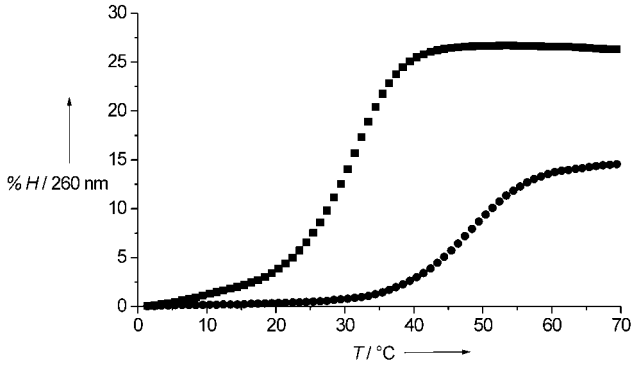

Figure 2. UV melting curves of the duplexes bca(GAGACCCGT)·bca(ACGGGTCTC) (squares) and d(GAGACCCGT)·d(ACGGGTCTC) (circles). Experimental conditions as indicated in Table 2.

As can be seen, bicyclo[3.2.1]amide-DNA forms duplexes not only in the homobasic A/T series, but also in a mixed-base context. With the nonsymmetric nonamer sequences **7**–**9** we could clearly show that antiparallel strand alignment (Table 2, entry 1) leads to stable duplexes, while parallel strand alignment within the same sequence context failed to produce a duplex (Table 2, entry 2). The thermal stability of bca-duplexes is diminished by 1.0–1.8 K per base-pair, relative to DNA. The reduced thermodynamic stability of the duplexes is not of enthalpic, but of entropic origin, as can be seen from the vant'Hoff transition enthalpies (ΔH).

From these data we conclude that elongation of the distance between base and backbone by one atom is still compatible with Watson–Crick duplex formation in short oligomers ($\ll$10 base-pairs). As in the case of DNA, duplex formation is restricted to antiparallel strand alignment, although bca-DNA shows enhanced structural flexibility in the attachment of the bases to the backbone units. This selectivity indicates a high degree of stereochemical control over duplex formation imposed by the structurally preorganized backbone. The thermodynamic data are in agreement with no additional strain in the complex, compared to DNA, but with reduced affinity due to the increased flexibility of the base-carrying unit.

CD spectroscopic investigation of the DNA and bca-DNA duplexes corresponding to entries 1 and 4 (Table 2) led to a surprise (Figure 3). The CD traces of the two duplexes are virtually enantiomorphic, indicating a left-handed Watson–Crick base-paired structure for the bca-NA duplex. Thus, the preference for left-handed duplex formation, as already observed in the A/T-homobasic bca-DNA series,[22] seems not to be restricted to the homo-A/T sequence context.

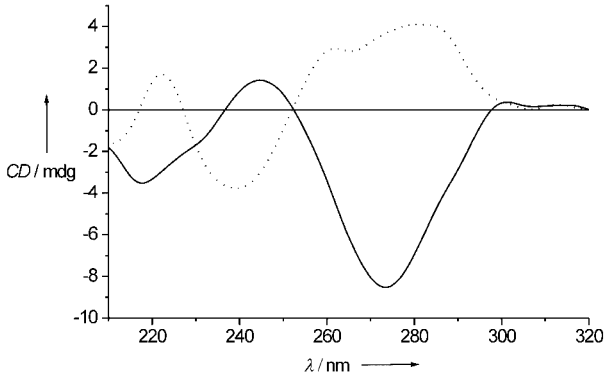

Figure 3. CD spectra (5 °C) of bca(GAGACCCGT)·bca(ACGGGTCTC) (solid line) and d(GAGACCCGT)·d(ACGGGTCTC) (dotted line). Experimental conditions as indicated in Table 2.

Pairing properties with complementary DNA and RNA in the mixed-base sequence series: Heterobackbone duplex formation between the mixed-sequence bca-oligonucleotides **7**–**9** and complementary DNA and RNA was analyzed in a similar way by UV melting curve analysis. The corresponding thermodynamic and T_m data are reproduced in Table 3. Bca oligonucleotides of mixed sequence do base-pair to antiparallel complementary DNA, with thermal affinity reduced by approximately 2.8 K per base pair (entries 1, 2). No duplex formation occurs with parallel oriented DNA complements (entry 3). In contrast to the homobackbone series (Table 2),

Table 3. T_m and thermodynamic data of duplex formation for mixed bca/DNA and bca/RNA duplexes.[a]

Entry		T_m[b]	ΔH [kJ mol^{-1}]	ΔS [J K^{-1} mol^{-1}]	ΔG^{298K} [kJ mol^{-1}]
1	bca(GAGACCCGT) (CTCTGGGCA)d	23.7	−201.3	−566.6	−32.4
2	bca(ACGGGTCTC) (TGCCCAGAG)d	23.5	−198.8	−557.2	−32.7
3	bca(CTCTGGGCA) d(GAGACCCGT)	nd	–	–	–
4	bca(ACGGGTCTC) (UGCCCAGAG)r^D	nd	–	–	–
5	bca(CTCTGGGCA) r^D(GAGACCCGU)	nd	–	–	–
6	d(GAGACCCGT) (CTCTGGGCA)r^D	51.1	−296.1	−799.3	−57.8

[a] Buffer conditions: 10 mM Na cacodylate, 1 M NaCl, pH = 7.0, total oligonucleotide concentration = 5 μM [b] nd = not detected.

0947-6539/02/0823-5314 $ 20.00+.50/0 *Chem. Eur. J.* **2002**, *8*, No. 23

the destabilization in the bca-DNA/DNA duplexes is mostly enthalpic in origin, most likely expressing some structural strain within the hydrogen-bonded complex. Interestingly, no duplex formation was observed either with parallel or with antiparallel oriented RNA. Thus, bca-DNA shows a remarkable selectivity towards DNA in the mixed sequence context.

We investigated the duplex structure of **8** with its DNA complement (Table 3, entry 2) and found its CD trace again to be enantiomorphic to that of the DNA/DNA and the DNA/RNA duplex (Figure 4).

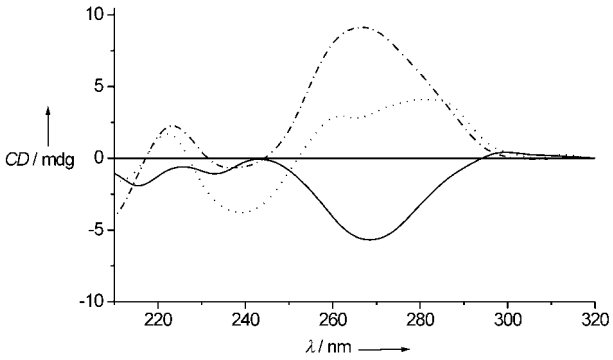

Figure 4. CD spectra (5 °C) of the duplexes bca(ACGGGTCTC)·d(GAGACCCGT) (solid line), d(GAGACCCGT)·d(ACGGGTCTC) (dotted line), and d(GAGACCCGT)·r^D(ACGGGUCUC) (dash-dotted line).

This behavior is opposite to that in the homobasic A/T series, in which the CD spectra of bca(XA_{10})·d(T_{10})[22] and bca(XA_{10})·r^D(XT_{10}) (Figure 5) do not show inversion of sign in their CD spectra although both contain a DNA or RNA complement. It thus emerges that, in a mixed-base context, bca-DNA can drive a complementary DNA strand into an enantiomorphic duplex conformation.

Pairing properties of homobasic A/T bca-DNA with D- and L-RNA: The picture becomes different in the homo-A/T sequences. As we noted earlier, no complementary base-pairing is observed for the bca-pyrimidine oligonucleotide **11** with DNA and RNA. Oligonucleotide **10**, on the other hand, was found to form duplexes both with complementary DNA and with complementary RNA (poly-U).[22] The particular observation that duplexes containing bca-DNA can adopt two enantiomorphic forms was intriguing enough to explore whether bca-DNA has the potential to form duplexes with both L- and D-configured RNA. Because no stable bca-DNA/RNA duplex occurred in the mixed-base sequence series, we investigated these features in the homobasic A/T-sequence series (Table 4).

Inspection of the data in Table 4 reveals that, indeed, oligonucleotide **10** forms duplexes with both the D- and the L-RNA complement. The difference in thermal stability is rather small (1 K per base pair) and underlines the chiral degeneracy of **10** in complementary strand recognition. A CD spectroscopic investigation on the structure of the homo- and heterochiral duplexes showed a typical right-handed Watson–Crick helix in the case of r^D(T_{10})X, and a left-handed helix in the case of r^L(T_{10})X as the complement (Figure 5).

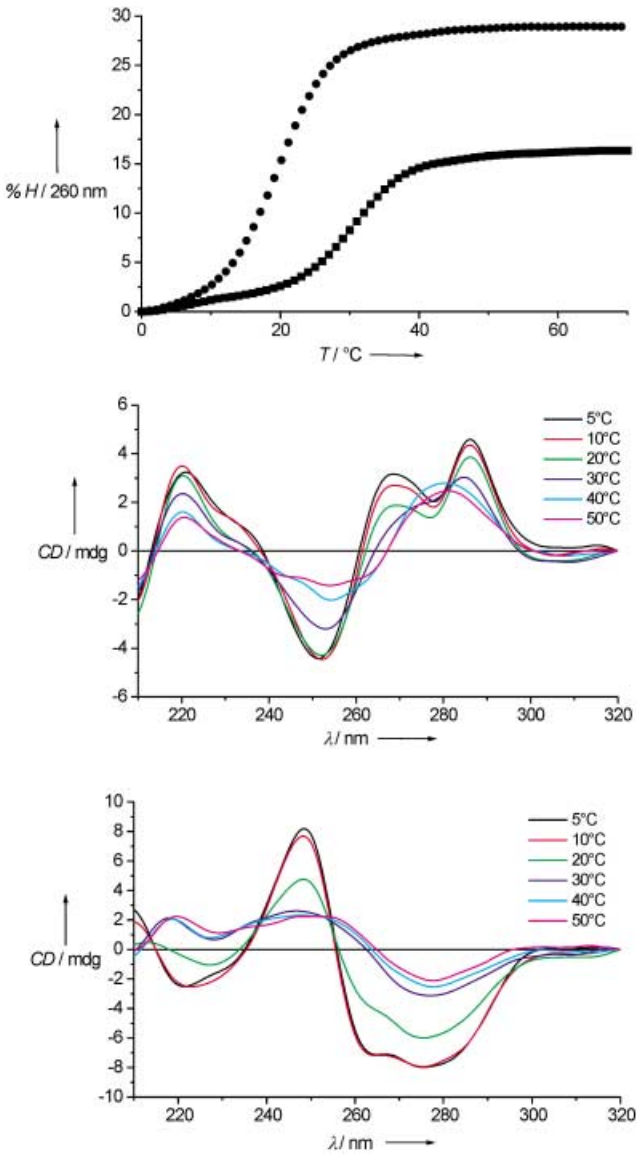

Figure 5. Top: UV melting curves of bca(XA_{10})·r^D(T_{10})X (squares) and bca(XA_{10})·r^L(T_{10})X (circles); middle: CD spectra of bca(XA_{10})·r^D(T_{10})X; bottom: CD spectra of bca(XA_{10})·r^L(T_{10})X; buffer conditions: 10 mM Na cacodylate, 1M NaCl, pH 7.0, total oligonucleotide concentration = 5 μM.

Table 4. T_m and thermodynamic data of duplex formation for bca/r^D and bca/r^L and the corresponding DNA/r^D and DNA/r^L duplexes.[a]

Entry		T_m[b]	ΔH [kJ mol^{-1}]	ΔS [J K^{-1} mol^{-1}]	$\Delta G^{298\,K}$ [kJ mol^{-1}]
1	bca(XA_{10})/ r^D(T_{10})X	30.7	−228.2	−637.0	−38.3
2	bca(XA_{10})/ r^L(T_{10})X	20.1	−316.5	−966.0	−28.5
3	d(A_{10})/ r^D(T_{10})X	37.0	na[c]	na[c]	na[c]
4	d(A_{10})/ r^L(T_{10})X	nd	–	–	–

[a] Buffer conditions: 10 mM Na cacodylate, 1M NaCl, pH 7.0, total oligonucleotide concentration = 5 μM. [b] nd = not detected. [c] na = not analyzed.

Thus, in contrast to the mixed sequences investigated before, bca oligonucleotide **10** can be accommodated in both a left- and a right-handed double helix. A plot of the relative stoichiometry of strands against absorption at constant oligonucleotide concentration (Job plot) in the homo- and

  0947-6539/02/0823-5315 $ 20.00+.50/0

heterochiral duplexes clearly indicated duplex formation and ruled out triplex formation under the experimental conditions applied (Figure 6).

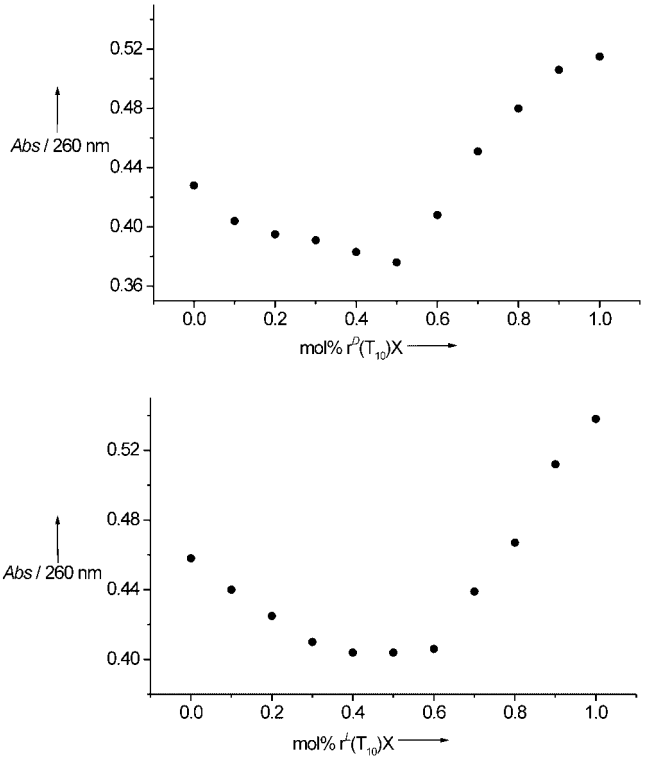

Figure 6. Job plots of bca(XA_{10}) with $r^D(T_{10})X$ (top), and with $r^L(T_{10})X$ (bottom) in 10 mM Na cacodylate, 1M NaCl, pH 7.0 at 5 °C. c(tot.) = 5 μM.

Interestingly, the thermodynamic data of duplex formation show a more favorable enthalpy term in the case of the heterochiral duplex than in that of the homochiral duplex. Thus it appears that bca-DNA shows enthalpic advantages in duplex formation whenever its complement intrinsically prefers left-handedness (L-RNA, bca-DNA) and a relative enthalpic disadvantage when the complement prefers right-handedness (DNA, D-RNA). As expected, the free enthalpies of duplex formation (ΔG) reflect the thermal stabilities inferred from the T_m values in any of the cases investigated (Table 4).

Molecular modeling: The unexpected, free and easy, structural accommodation of the homochiral bca-DNA backbone in both a left- and a right-handed double-helix in the homo-A/T series is unique, and prompted us to search for relevant structural parameters. It is evident that the conformational flexibility of the backbone resides in the two bridging P–O bonds, and in the adjacent O–C(3′), O–C(5′) bonds. In the base linker unit, conformational diversity occurs around the C–N bond and (to a lesser extent) around the O=C–C–N(base) bond. From the three possible staggered conformations around the C–N bond in a bca-nucleoside monomer, it appears that the *endo*[3.2] conformer (in which the carbonyl oxygen of the base-linker unit lies in-between the three- and the two-center bridges of the bicyclo scaffold) and the *endo*[3.1] conformer are slightly more stable than the *endo*[2.1] conformer, by about 1 – 1.5 kcal mol^{-1} (Figure 7).

An extension of the *endo*[3.2] and the *endo*[3.1] conformers to the dimer level opens the possibility of inter-residue hydrogen-bond formation between the base-linker amide functions of two consecutive nucleotide residues. By constraining the phosphodiester backbone in a B-DNA geometry, the *endo*[3.1] conformer is intrinsically preorganized for right-handed helix formation and the *endo*[3.2] conformer for left-handed helix formation (Figure 8).

With this as the background we modeled the three different antiparallel, duplexes bca(A_{10})·bca(T_{10}), bca(A_{10})·$r^L(T_{10})$, and bca(A_{10})·$r^D(T_{10})$ (Figure 9; see Experimental Section). Indeed, the two left- and the right-handed duplex structures also show uninterrupted base-pairing after unconstrained energy minimization. All structures show a spine of hydrogen bonds along the base-linker units in the bca-DNA strands. In the right-handed bca(A_{10})·$r^D(T_{10})$ duplex (Figure 9) the r^DT strand completely conserves its native backbone geometry, while the bca-DNA strand shows the base-linker C–N bonds in the *endo*[3.1] conformation. The left-handed bca(A_{10})·$r^L(T_{10})$ duplex (Figure 9) shows the r^LT strand in an almost perfect mirror image conformation with respect to the r^DT backbone. The bca(A_{10}) strand almost exclusively uses the described amide switch from the *endo*[3.1] to the *endo*[3.2] conformation in order to accommodate itself in both helical forms.

Most interestingly, the backbone torsion angles $\alpha - \zeta$ in the bca-DNA strands are very similar in both the left- and the right-handed duplex. The switch from the right- to the left-handed duplex (Figure 9) is operated through sign changes of all of the backbone torsional angles for the oligoribothymi-

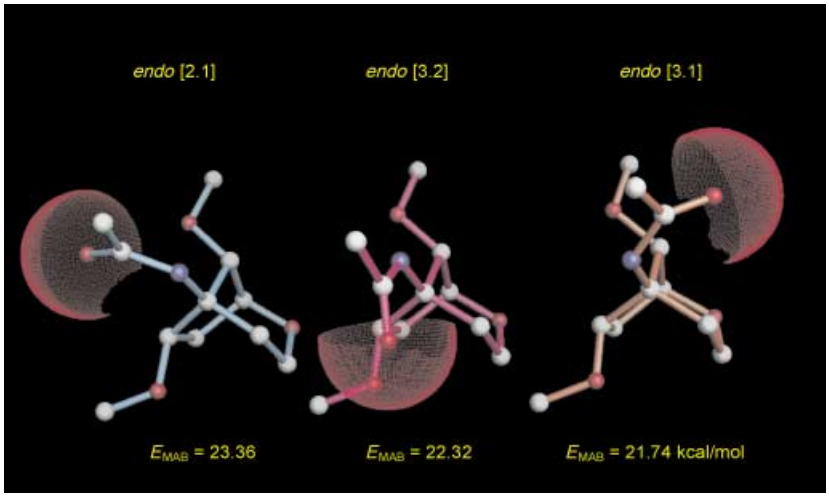

Figure 7. Conformational analysis of the bridgehead amide orientation in an isolated bicyclo[3.2.1]-NA backbone unit. The bases are omitted for clarity.

0947-6539/02/0823-5316 $ 20.00+.50/0 *Chem. Eur. J.* **2002**, *8*, No. 23

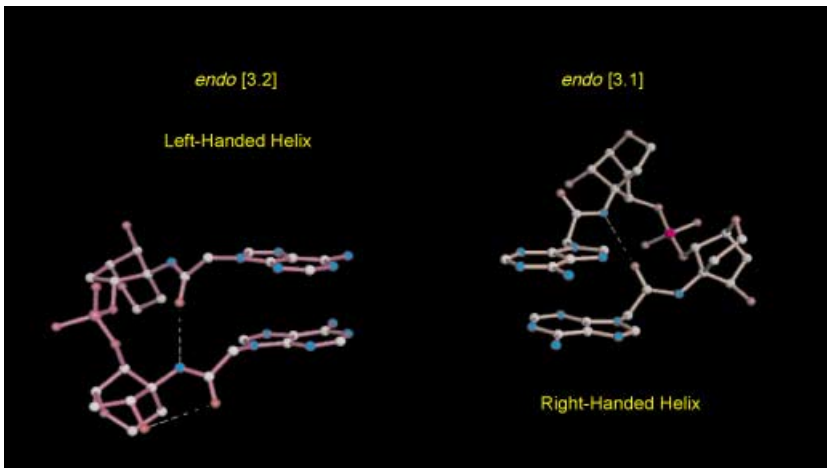

Figure 8. Representation of a bca-dinucleotide unit in both helical conformations, as determined by molecular modeling. The bases are held in place by inter-residue hydrogen bonds.

dine strand, but only very subtle ($\pm 25^\circ$) changes of the angles α and ζ for the bicyclo[3.2.1]amide backbone (Table 5). Remarkably, the geometries are very consistent for the modified backbone strands when proceeding from the hetero- to the homoduplex.

Bca strands use the intermediate amide function as a relay to switch between a right- and a left-handed conformation. This relay leads to almost superimposable sugar units but enantiomorphically arranged bases, as can be seen from Figure 10, which displays a bca-A unit out of a left- and a right-handed double helix.

Discussion

Besides bicyclo[3.2.1]-DNA (Figure 1),[14–16] there were only a few other known DNA analogues in which the bases are linked to a phosphodiester backbone through a non-cyclic unit. These are glycerol-DNA,[11] the *seco*-DNAs,[9, 10] and inverse DNA.[23] While fully modified single strands of the former two systems are known to be incompetent in duplex formation, no data on fully modified strands are available in the case of inverse DNA. With respect to bicyclo[3.2.1]-DNA, in which the number of bonds (three) between the base unit and the backbone is identical to that in DNA, the following common properties were found for bicyclo[3.2.1]amide-DNA, in which the base is more distant by one bond (four in total) from the backbone. Both systems base-pair to themselves and to complementary DNA with reduced affinity relative to DNA. Both systems show strong preferences for antiparallel strand alignment in duplexes and show strong discrimination of base-mismatch formation. Two evident differences are the complementary base-pairing with RNA and the structural differences as observed by CD spectroscopy. In a mixed-base sequence context, bca oligonucleotides show highly reduced affinity for complementary RNA, which is not the case for the bicyclo[3.2.1]-DNA. In contrast to bca oligonucleotides, there were no signs of left-handed duplex formation by bicyclo[3.2.1]-oligonucleotides with either DNA or RNA. Whether the latter system may cross-pair with enantio-RNA, as bca oligonucleotides do, has not been investigated so far.

Thus, it appears that elongation of the linker between the base and a preorganized backbone facilitates the formation of left-handed duplex structures and, hence, promotes the loss of chiroselectivity. An inspection of available data shows that promiscuous heterochiral strand recognition occurs in a number of oligonucleotidic systems, but is typically much weaker than homochiral strand recognition. For example, it has been shown that enantiomeric homodeoxyadenylates can bind to poly(U).[24] This, however, seems to be an exception as, in a mixed base context, recognition of DNA and RNA by L-DNA does not occur.[25] It has also been shown that oligo-homothymidylates of the RNA analogue LNA can bind to complementary L-RNA, forming enantiomorphic duplex structures.[26] The cyclohexanyl DNA analogue CNA (the carba analogue of the hexitol nucleic acid analogue HNA) forms heterochiral duplexes in its own series (homo-A/homo-T strands) but not with DNA and RNA.[5] The same feature is known for the RNA isomer pRNA, which can form heterochiral duplexes within its backbone type in a non-natural base-context,[27] but typically has a strong preference for homochiral duplex formation.[28]

Inspection of the backbone torsion angles of bca strands in left- and right-handed duplexes, as obtained from molecular modeling, highlights the relative ease with which the helicity of a duplex can be inverted by minor structural changes in the phosphodiester backbone. While torsion angles γ and δ are invariant for obvious reasons, changes of torsion angles α and ζ of less than 25° can induce inversion of handedness of the backbone. The attachment of the bases to the backbone through a cyclic structural element (such as the ribofuranose unit of DNA and RNA) seems to be a measure to increase enantiodifferentiation in duplex formation, as it constrains the attainable conformational space of the nucleobases and reduces the possibility of enantiomorphic arrangements of the bases in a manner such as displayed in Figure 10.

There is a pronounced difference in the thermal stabilities of duplexes of homobasic against mixed-base bicyclo[3.2.1]-amide-DNA. In the mixed-base context, bca/bca duplexes are more stable than bca/DNA duplexes, while bca/RNA duplex formation has not been observed. In the homobasic (A/T) context, only the purine bca oligonucleotides form duplexes with complementary DNA and RNA with thermal stabilities relatively similar to those of the duplex consisting of two bca strands. Whatever the molecular basis of this differential behavior might be, triple-helix formation in the homopurine/homopyrimidine system can be excluded as a potential cause, from the corresponding Job plots (Figure 6).

  0947-6539/02/0823-5317 $ 20.00+.50/0

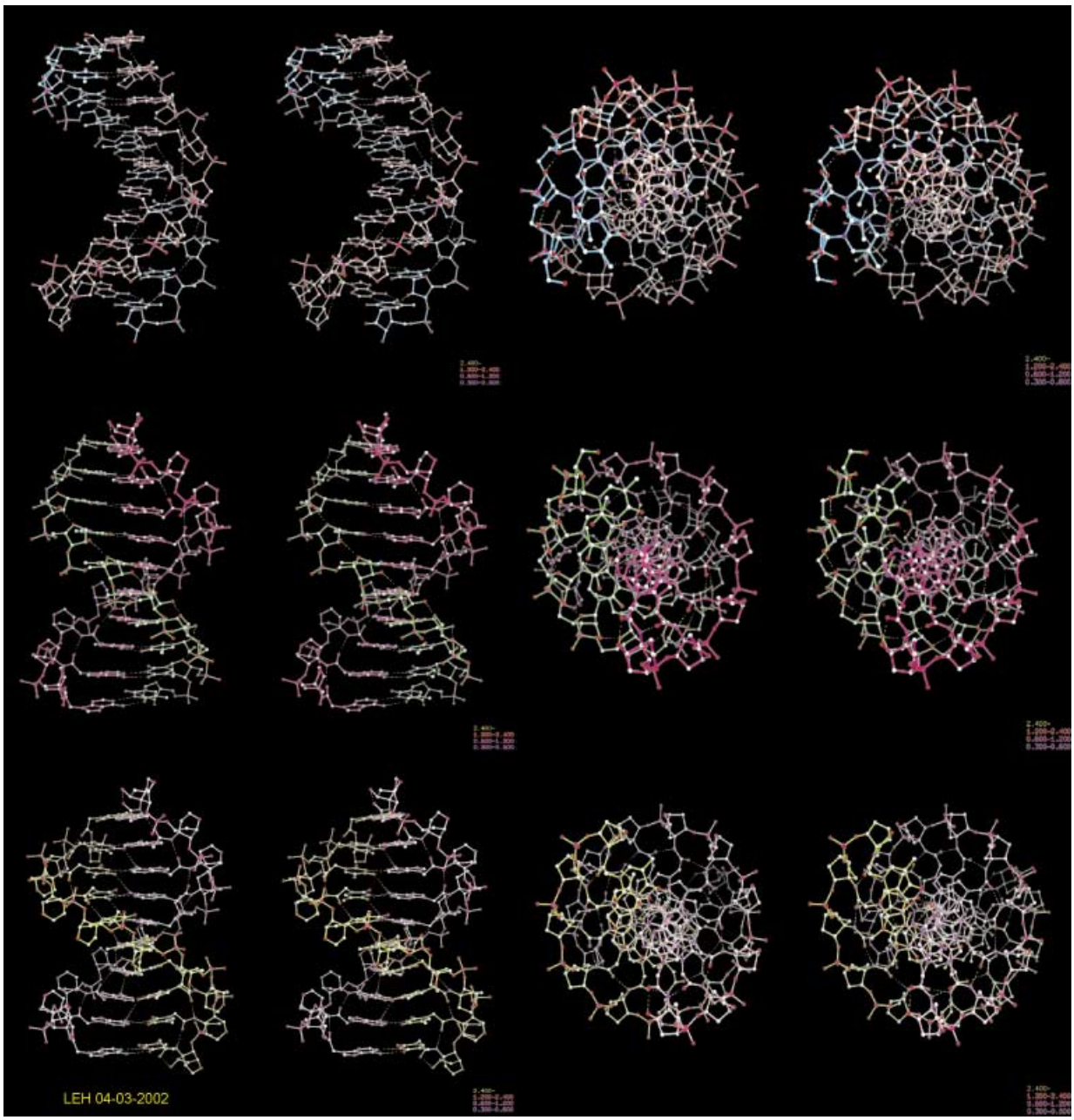

Figure 9. Stereoview of duplexes perpendicular and parallel to the helix axis. Top: right-handed bca(A_{10})·r^D(T_{10}); middle: left-handed bca(A_{10})·r^L(T_{10}); bottom: left-handed bca(A_{10})·bca(T_{10}).

Table 5. Backbone torsional angles[a] [°] for the three duplexes indicated, obtained from molecular modeling.

	Torsion angle	bca(A_{10})·bca(T_{10})	bca(A_{10})·r^D(T_{10})	bca(A_{10})·r^L(T_{10})
A strand	α	−37 (−*sc*)	−10 (−*sc*)	−35 (−*sc*)
	β	+160 (+*ap*)	+162 (+*ap*)	+159 (+*ap*)
	γ	+68 (+*sc*)	+68 (+*sc*)	+68 (+*sc*)
	δ	+157 (+*ap*)	+157 (+*ap*)	+157 (+*ap*)
	ε	+126 (+*ac*)	+127 (+*ac*)	+124 (+*ac*)
	ζ	−145 (−*ac*)	−134 (−*ac*)	−146 (−*ac*)
T strand	α	−36 (−*sc*)	−61 (−*sc*)	+63 (+*sc*)
	β	+159 (+*ap*)	+158 (+*ap*)	−159 (−*ap*)
	γ	+68 (+*sc*)	+60 (+*sc*)	−61 (−*sc*)
	δ	+157 (+*ap*)	+86 (+*sc*)	−85 (−*sc*)
	ε	+127 (+*ac*)	−159 (−*ap*)	+160 (+*ap*)
	ζ	−146 (−*ac*)	−79 (−*sc*)	+76 (+*sc*)

[a] *sc* = synclinal, *ac* = anticlinal, *ap* = antiperiplanar.

Bicyclo[3.2.1]amide-DNA has some structural similarity with the polyamide nucleic acid analogue PNA,[29–31] as it shares the same base linker unit with PNA. While it is evident that PNA, due to its achiral nature, can be accommodated in right- and left-handed double helices, it appears that PNA is somewhat less selective, in that antiparallel and parallel duplex formation with complementary DNA and RNA can be observed, this in spite of the fact that there is no change in the backbone-to-base distance (three bonds) relative to DNA. In terms of antisense applications, however, bicyclo[3.2.1]amide-DNA is not competitive relative to PNA as it discriminates RNA binding and shows overall reduced affinity to DNA.

The linker amide functions in bca oligonucleotides offer the possibility of inter-residue hydrogen-bond formation. During molecular modeling (Figure 8, Figure 9) such hydrogen bonds

0947-6539/02/0823-5318 $ 20.00+.50/0 *Chem. Eur. J.* **2002**, *8*, No. 23

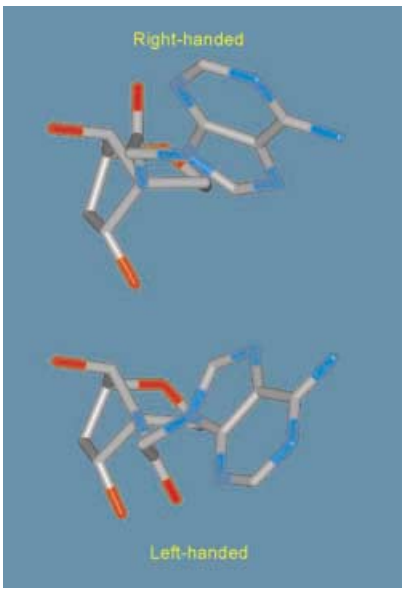

Figure 10. Representation of a bca-A unit in the right- (top) and left-handed (bottom) helical conformation. While the backbone bonds of the two units are almost superimposable, the bases adopt enantiomorphic positions.

were spontaneously formed in both the right- and the left-handed duplex structures. In principle, such a hydrogen-bond network between consecutive base elements could ideally add to the preorganization of single strands for duplex formation. An NMR structural investigation of a bca-(AT) dimer, however, has not so far provided compelling evidence that such a hydrogen-bonding network exists in solution (data not shown). A definitive answer to this question requires a detailed structural analysis of a stable duplex. As a note of caution we add that intra- and inter-residue hydrogen-bond formation in PNA, involving the base-linker amide function, has been proposed on the basis of molecular modeling,[32, 33] but has never been observed in high-resolution structures of PNA duplexes and triplexes.[34, 35]

Previous studies on DNA analogues have shown that the number of bonds in the repetitive DNA backbone can be varied to five[12, 36] or seven[7] without breakdown of complementary recognition of RNA and DNA. Bicyclo[3.2.1]amide-DNA is the first analogue to demonstrate that the distance between the base and the backbone can also be extended from three to four bonds without breakdown of complementary Watson–Crick base-pairing.

Experimental Section

General: Reactions were carried out under Ar in distilled, anhydrous solvents. 2-Cyanoethyl *N*,*N*-diisopropylchlorophosphoramidite was from Sigma and 4,4′-(dimethoxytriphenyl)methyl triflate (DMT-OTf) was prepared as described.[37] All other reagents were from Fluka (highest quality available). All NMR spectra were measured at room temperature. ^{1}H NMR spectra: δ in ppm relative to solvent ([D]chloroform = 7.24, [D$_6$]DMSO = 2.49, or [D$_6$]benzene = 7.20), J in Hz. ^{13}C NMR spectra: δ in ppm relative to solvent ([D]chloroform = 77.00, [D$_6$]DMSO = 39.70, or [D$_6$]benzene = 128.00), multiplicities from DEPT spectra. ^{31}P NMR spectra: δ in ppm relative to 85% H_3PO_4 as external standard). ESI-MS: VG platform Fisons instruments. LSI-MS: Micromass Autospec Q VG. TLC: pre-coated plates SIL-G-25 UV254 (Machery–Nagel). Visualization by UV and/or by dipping into a solution of $Ce(SO_4)_2$ (10.5 g), phosphomolybdic acid (21 g), H_2SO_4 (60 mL), and H_2O (900 mL). Flash chromatography: silica gel 60 (230–400 mesh).

Compound 3a: *O*-[(Ethoxycarbonyl)-cyanomethylene-amino]-*N*,*N*,*N*′,*N*′-tetramethyluronium tetrafluoroborate (TOTU) (36 mg, 0.11 mmol) was added at room temperature to a solution of **1** (30 mg, 0.11 mmol), (iPr)$_2$NEt (0.1 mL), and **2a** (36 mg, 0.11 mmol) in DMF (5 mL). After stirring overnight the mixture was concentrated (HV, 40 °C) and extracted (AcOEt/sat. $NaHCO_3$). Purification by flash chromatography (AcOEt) gave **3a** (56 mg, 88%) as a white solid. R_f = 0.61 (EtOAc); ^{1}H NMR (300 MHz, [D]chloroform, 25 °C): δ = 0.07, 0.11 (2s, 6H; $(CH_3)_2$Si), 0.88 (s, 9H; $(CH_3)_3$C), 1.36 (s, 9H; $(CH_3)_3$CPh), 1.64 (m, 1H; C(7)H), 1.84 (m, 1H; C(4)H), 2.42 (dd, ^3J(H,H) = 12.5, 3.7 Hz, 1H; C(4)H), 2.59 (ddd, ^3J(H,H) = 15.8, 10.7, 5.9 Hz, 1H; C(7)H), 3.65 (dd, ^3J(H,H) = 11.8, 6.6 Hz, 1H; C(3)H), 3.83 (s, 1H; C(8)H), 4.04–4.16 (m, 1H; C(1)H, 1H; C(3)H), 4.36, 4.62 (2d, ^3J(H,H) = 14.3 Hz, 2H; CH_2), 4.45–4.48 (m, 1H; C(6)H), 4.64 (s, 1H; C(6)OH), 6.91 (s, 1H; NH), 7.53 (d, ^3J(H,H) = 8.5 Hz, 2H; ArH), 7.65 (d, ^3J(H,H) = 7.4 Hz, 1H; ArH), 7.73 (d, ^3J(H,H) = 7.4 Hz, 1H; ArH), 7.81 (d, ^3J(H,H) = 8.5Hz, 2H; ArH), 8.64 ppm (s, 1H; NH); ^{13}C NMR (75 MHz, [D]chloroform, 25 °C): δ = −5.05, −4.48 (2q), 17.80 (s), 25.58, 31.02 (2d), 31.58, 34.76 (2t), 35.16, 38.57 (2s), 53.50, 59.29 (2t), 66.53 (s), 75.41, 78.56, 80.86, 97.36 (4d), 126.06, 127.50 (2q), 129.73 (s), 149.19 (d), 157.33, 163.01, 168.01 ppm (3s); HRMS, ESI-MS calcd for $C_{30}H_{44}N_4O_6Si$: 583.2958; found: 583.2971 [M^- − H].

Compound 3b: This compound was prepared as described for **3a**, from **1** (192 mg, 0.71 mmol), **2b** (238 mg, 0.44 mmol), and TOTU (258 mg, 0.78 mmol) in DMF (5 mL). Compound **3b** (390 mg, 81%) was obtained after flash chromatography (AcOEt → AcOEt/MeOH 9:1) as a white solid. This material was used without characterization for the next step.

Compound 3c: This compound was prepared as described for **3a**, from **1** (195 mg, 0.71 mmol), **2c** (270 mg, 0.99 mmol), and TOTU (270 mg, 0.82 mmol) in DMF (10 mL). Compound **3c** (227 mg, 60%) was obtained after flash chromatography (MeOH/CH_2Cl_2 1:9) as a white solid. R_f = 0.34 (MeOH/CH_2Cl_2 = 1:9); ^{1}H NMR (300 MHz, [D$_6$]DMSO, 25 °C): δ = −0.11, −0.03 (2s, 6H; $(CH_3)_2$Si), 0.82 (s, 9H; $(CH_3)_3$Si), 1.10 (d, ^3J(H,H) = 6.6 Hz, 6H; 2CH_3,), 1.49 (dd, ^3J(H,H) = 16.1, 1.8 Hz, 1H; C(7)H), 1.63 (dd, ^3J(H,H) = 12.5, 3.3 Hz, 1H; C(4)H), 2.28 (m, 1H; C(4)H, 1H; C(7)H), 2.76 (sept, ^3J(H,H) = 7.0 Hz, 1H; CH), 3.51 (dd, ^3J(H,H) = 11.0, 6.6 Hz, 1H; (3)H), 3.78 (d, ^3J(H,H) = 5.5 Hz, 1H; C(1)H), 4.18 (s, 1H; C(8)H), 4.20–4.24 (m, 1H; C(6)H), 4.73 (s, 2H; CH_2CO), 4.98 (d, ^3J(H,H) = 4.1, 1H; C(6)OH), 7.75 (s, 1H; NH), 8.16 (s, 1H; CH), 11.62, 12.05 ppm (2s, 2H; NH); ^{13}C NMR (75 MHz, [D$_6$]DMSO, 25 °C): δ = −4.90, −4.88 (2q), 17.69 (s), 18.95, 19.20, 25.75 (3q), 30.21, 34.54 (2t), 34.86 (d), 45.50, 58.79 (2t), 65.14 (s), 73.86, 78.03, 78.40 (3d), 119.69 (s), 140.79 (d), 148.03, 149.18, 155.06, 165.97, 180.28 ppm (5s); HRMS, LSI-MS calcd for $C_{24}H_{39}N_6O_6Si$: 535.2697; found: 535.2700 [M^++H].

Compound 3d: This compound was prepared as described for **3a**, from **1** (100 mg, 0.36 mmol), **2d** (84 mg, 0.46 mmol), and TOTU (132 mg, 0.40 mmol) in DMF (5 mL). Compound **3d** (128 mg, 76%) was obtained after flash chromatography (AcOEt → AcOEt/MeOH 9:1), as a white solid. R_f 0.18 (AcOEt/$CHCl_3$ 9:1); $[\alpha]_D^{25}$ = −16.40 (c = 0.5 in $CHCl_3$); ^{1}H NMR (300 MHz, [D$_6$]DMSO, 25 °C): δ = −0.03, −0.01 (2s, 6H; $(CH_3)_2$Si), 0.81 (s, 9H; $(CH_3)_3$C), 1.49 (dd, ^3J(H,H) = 15.1, 1.8 Hz, 1H; C(7)H), 1.66 (dd, ^3J(H,H) = 12.5, 3.5 Hz, 1H; C(4)H), 1.73 (d, ^4J(H,H) = 1.1 Hz, 3H; CH_3), 2.21 (dt, ^3J(H,H) = 12.1, 7.0 Hz, 1H; C(4)H), 2.31 (ddd, ^3J(H,H) = 16.2, 10.3, 5.9 Hz, 1H; C(7)H), 3.51 (dd, ^3J(H,H) = 11.4, 7.0 Hz, 1H; C(3)H), 3.78 (dt, ^3J(H,H) = 12.1, 3.7 Hz, 1H; C(3)H), 3.86 (dd, ^3J(H,H) = 5.5, 1.1 Hz, 1H; C(1)H), 4.13 (s, 1H; C(8)H), 4.19–4.24 (m, 1H; C(6)H), 4.24, 4.30 (2d, ^3J(H,H) = 16.2 Hz, 2H; CH_2CO), 4.93 (d, ^3J(H,H) = 3.3 Hz, 1H; C(6)OH), 7.30 (s, 1H; NH), 8.06 (s, 1H; CH), 11.23 ppm (s, 1H; NH); ^{13}C NMR (75 MHz, [D]chloroform, 25 °C): −5.08, −4.48, 12.42 (3q), 17.80 (s), 25.53 (q), 31.96, 34.78, 51.29, 59.20 (4t), 66.67 (s), 75.13, 78.41, 81.05 (3d), 111.4 (s), 140.79 (d), 151.07, 164.34, 168.32 ppm (3s); HRMS, LSI-MS calcd for $C_{20}H_{34}N_3O_6Si$: 440.2217; found: 440.2227 [M^++H]; elemental analysis calcd (%) for $C_{20}H_{33}O_6SiN_3 \cdot 1.25\,H_2O$ (462.10): C 51.98, H 7.43, N 9.09; found C 51.89, H 7.19, N 8.80.

Compound 4a: DMT-OTf (154 mg, 0.34 mmol) was added at room temperature to a solution of **3a** (100 mg, 0.17 mmol) in pyridine (0.9 mL). The reaction mixture was stirred at 60 °C. An additional 1 equiv

  0947-6539/02/0823-5319 $ 20.00+.50/0

(76 mg, 0.17 mmol) of DMT-OTf was added in two portions over 3 h. After 5 h the mixture was extracted (AcOEt/sat. $NaHCO_3$), the organic phase was evaporated, and the residue was purified by flash chromatography (EtOAc/hexane 1:2 → 1:1) to give **4a** (131 mg, 87%) as a pale yellow solid. $R_f = 0.30$ (AcOEt/hexane 1:2, silica gel pre-deactivated by 1% TEA in hexane); ^{1}H NMR (300 MHz, [D$_6$]benzene, 25 °C): $\delta = -0.10, 0.02$ (2s, 6H; $(CH_3)_2Si$), 0.81 (s, 9H; $(CH_3)_3C$), 1.19 (s, 9H; $(CH_3)_3CPh$), 1.58 (d, $^3J(H,H) = 15.1$ Hz, 1H; C(7)H), 1.81 (ddd, $^3J(H,H) = 15.1$, 10.0, 5.9 Hz, 1H; C(7)H), 2.30 (m, 1H; C(4)H), 3.04 (dt, $^3J(H,H) = 12.5$, 7.3 Hz, 1H; C(4)H), 3.48, 3.44 (2s, 6H; $2CH_3$), 3.90 (dd, $^3J(H,H) = 11.0$, 7.0 Hz, 1H; C(3)H), 4.01 (d, $^3J(H,H) = 5.1$ Hz, 1H; C(1)H), 4.13, 4.37 (2d, $^3J(H,H) = 14.7$ Hz, 2H; CH_2), 4.32 (m, 1H; C(6)H), 4.43 (m, 1H; C(3)H), 4.70 (s, 1H; C(8)H), 5.99 (s, 1H; NH), 6.91 (m, 4H; ArH), 7.14 (d, $^3J(H,H) = 7.3$ Hz, 2H; ArH), 7.31 (m, 4H; ArH), 7.42 (d, $^3J(H,H) = 7.2$ Hz, 2H; ArH), 7.56 (m, 5H; ArH), 7.72 (d, $^3J(H,H) = 7.7$Hz, 2H; ArH), 8.06 (d, $^3J(H,H) = 7.7$ Hz, 2H; ArH), 9.68 ppm (s, 1H; NH); ^{13}C NMR (75 MHz, [D$_6$]benzene, 25 °C): $\delta = -4.94, -4.83$ (2q), 17.90 (s), 25.87, 31.02 (2q), 31.19, 34.02 (2t), 34.90 (s), 52.86 (t), 54.88, 54.95 (2q), 59.98 (t), 66.58 (s), 77.23, 78.38, 78.97 (3d), 87.31 (s), 113.77, 113.94, 125.87, 127.29, 128.34, 128.81, 131.04, 131.25 (8d), 136.75, 137.12, 146.75 (3s), 150.05 (d), 156.18, 159.40, 159.42, 163.54, 166.21 ppm (5s); HRMS, LSI-MS calcd for $C_{51}H_{62}N_4O_8Si$: 887.4422; found: 887.4415 [M^++H].

Compound 4b: This compound was prepared as described for **4a**, from **3b** (390 mg, 0.71 mmol) and DMT-OTf (930 mg, 2.02 mmol) in pyridine (4 mL) overnight. Compound **4b** (415 mg, 69%) was obtained as a white solid after flash chromatography (AcOEt/CH_2Cl_2 9:1). $R_f = 0.34$ (AcOEt/CH_2Cl_2 9:1); $[\alpha]_D^{25} = +10.43$ ($c = 0.58$ in $CHCl_3$); ^{1}H NMR (300 MHz, [D]chloroform, 25 °C): $\delta = -0.26, -0.12$ (2s, 6H; $(CH_3)_2Si$), 0.67 (s, 9H; $(CH_3)_3C$), 1.48 (d, $^3J(H,H) = 15.4$ Hz, 1H; C(7)H), 1.75 (ddd, $^3J(H,H) = 15.8, 9.1, 5.1$ Hz, 1H; C(7)H), 2.04 (dd, $^3J(H,H) = 12.9, 3.7$ Hz, 1H; C(4)H), 2.64 (dt, $^3J(H,H) = 12.9$, 7.4 Hz, 1H; C(4)H), 3.81 (brs, 6H; $2CH_3$, 1H; C(3)H), 4.13–4.22 (m, 1H; C(3)H), 4.3 (s, 1H; C(8)H), 4.37, 4.54 (2d, $^3J(H,H) = 16.2$ Hz, 2H; CH_2), 5.10 (s, 1H; NH), 6.88–6.93 (m, 4H; ArH), 7.26–7.61 (m, 12H; ArH), 7.98–8.01 (m, 2H; ArH), 8.07, 8.69 (2s, 2H; 2CH), 9.06 ppm (brs, 1H; NH); ^{13}C NMR (75 MHz, [D]chloroform, 25 °C): $\delta = -5.31, -4.94$ (2q), 17.56 (s), 25.42 (q) 30.45, 33.69, 45.83 (3t), 55.22, 55.26 (2q), 59.60 (t), 66.29 (s), 76.39, 77.49, 78.50 (3d), 86.82 (2s), 113.35, 113.41 (2d), 122.15 (s), 127.21, 127.7, 128.02, 128.33, 128.75, 130.54, 130.65, 132.62 (8d), 133.71, 136.10, 136.51 (3s), 143.62(d), 145.54, 149.37, 151.86, 152.49, 158.84, 158.87, 164.03 ppm (7s); HRMS, LSI-MS calcd for $C_{48}H_{55}O_7N_6Si$: 855.3902; found: 855.3908 [M^++H].

Compound 4c: This compound was prepared as described for **4a**, from **3c** (235 mg, 0.44 mmol) and DMT-OTf (600 mg, 1.32 mmol) in pyridine (2.3 mL) overnight. Compound **4c** (202 mg, 55%) was obtained after flash chromatography (MeOH/EtOAc 1:9) as a pale yellow solid. $R_f = 0.70$ (MeOH/CH_2Cl_2 = 1:9, silica gel pre-deactivated by 1% TEA in hexane); ^{1}H NMR (300 MHz, [D$_6$]benzene, 25 °C): $\delta = -0.10, -0.01$ (2s, 6H; $(CH_3)_2Si$), 0.82 (s, 9H; $(CH_3)_3Si$), 1.19 (d, $^3J(H,H) = 6.6$ Hz, 6H; $2CH_3$), 1.62 (m, 1H; C(7)H), 1.86 (m, 1H; C(7)H), 2.42 (m, 1H; C(4)H), 2.91 (sept, $^3J(H,H) = 6.9$ Hz, 1H; $2CH_3$), 3.00 (m, 1H; (4)H) 3.54, 3.61 (2s, 6H; $2CH_3$), 3.93 (dd, $^3J(H,H) = 7.3$, 7.0 Hz, 1H; C(3)H), 4.01 (d, $^3J(H,H) = 5.2$ Hz, 1H; C(1)H), 4.40–4.52 (m, 1H; C(6)H, 1H; C(3)H), 4.60 (s, 1H; C(8)H), 4.76–4.90 (2d, $^3J(H,H) = 16.5$ Hz, 2H; CH_2CO), 5.83 (s, 1H; NH), 6.97 (m, 4H; ArH), 7.24 (d, $^3J(H,H) = 7.3$ Hz, 1H; ArH), 7.36 (t, $^3J(H,H) = 7.3$ Hz, 2H; ArH), 7.60 (t, $^3J(H,H) = 8.8$ Hz, 4H; ArH), 8.00 (s, 1H; CH), 10.54, 12.56 ppm (2s, 2H; NH); ^{13}C NMR (75 MHz, [D$_6$]benzene, 25 °C): $\delta = -4.98, -4.86$ (2q), 17.87 (s), 19.02, 19.20, 25.77 (3q), 31.90, 34.20 (2t), 36.08 (d), 46.49 (t), 55.06, 55.21 (2q), 60.03 (t), 66.79 (s), 77.68, 77.90, 78.87 (3d), 87.32 (s), 113.91, 113.79 (2d), 120.10 (s), 127.41, 128.33, 128.80, 131.02, 131.28 (5d), 136.81, 137.33 (2s), 141.03 (d), 146.75, 148.61, 149.75, 156.30, 159.37, 159.40, 165.62, 180.29 ppm (8s); HRMS, ESI-MS calcd for $C_{45}H_{55}N_6O_8Si$: 835.3856; found 835.3838 [M^- − H].

Compound 4d: This compound was prepared as described for **4a**, from **3d** (84 mg, 0.19 mmol) and DMT-OTf (240 mg, 0.53 mmol) in pyridine (0.9 mL) overnight. Compound **4d** (110 mg, 78%) was obtained after flash chromatography (Et_2O/MeOH 9:1) as a white solid. $R_f = 0.19$ ($CHCl_3$); $[\alpha]_D^{25} = +15.47$ ($c = 1.06$ in $CHCl_3$); ^{1}H NMR (300 MHz, [D$_6$]benzene, 25 °C): $\delta = -0.10, 0.01$ (2s, 3H; CH_3Si), 0.81 (s, 9H; $(CH_3)_3C$), 1.73 (s, 3H; CH_3), 1.73 (d, $^3J(H,H) = 9.9$ Hz, 1H; C(7)H), 1.96 (ddd, $^3J(H,H) = 15.5, 9.9, 5.5$ Hz, 1H; C(7)H), 2.22 (dd, $^3J(H,H) = 12.5, 3.7$ Hz, 1H; C(4)H), 3.04 (dt, $^3J(H,H) = 12.9, 7.0$ Hz, 1H; C(4)H), 3.47, 3.52 (2s, 6H; $2CH_3$), 3.46, 3.85 (2d, $^3J(H,H) = 15.8$ Hz, 2H; CH_2), 3.90 (dd, $^3J(H,H) = 11.4, 6.6$ Hz, 1H; C(3)H), 4.10 (d, $^3J(H,H) = 4.0$ Hz, 1H; C(1)H), 4.36 (dd, $^3J(H,H) = 9.9, 3.7$ Hz, 1H; C(6)H), 4.41 (dt, $^3J(H,H) = 11.8, 3.7$ Hz, 1H; C(3)H), 4.78 (s, 1H; C(8)H), 5.30 (s, 1H; NH), 6.42 (s, 1H; CH), 6.88–6.98 (m, 4H; ArH), 7.16–7.31 (m, 3H; ArH) 7.54–7.59 (m, 4H; ArH), 7.68–7.71 (m, 2H; ArH), 10.61 ppm (s, 1H; NH); ^{13}C NMR (75 MHz, [D$_6$]benzene, 25 °C): $\delta = -4.94$, 12.28 (2q), 17.90 (s), 25.78 (q), 31.23, 34.15, 49.98 (3t), 54.91, 54.99 (2q), 59.87 (t), 66.50 (s), 77.29, 78.25, 78.93 (3d), 87.40, 110.24 (2s), 113.70, 113.89, 127.35, 128.75, 131.07, 131.30 (6d), 136.58, 137.15 (2s), 140.64 (d), 146.66, 151.39, 159.48, 159.49, 164.22, 165.68 ppm (6s); FAB-MS: 780.20 [M^++K].

Compound 5a: Bu_4NF (24 mg, 0.076 mmol) was added at room temperature to a solution of **4a** (34 mg, 0.038 mmol) in THF (1 mL), and the mixture was stirred overnight. After evaporation of the solvent the crude product was purified by flash chromatography (CH_2Cl_2/MeOH = 10:1) to give **5a** (23 mg, 81%) as a pale yellow solid. $R_f = 0.24$ (AcOEt, silica gel pre-deactivated by 1% TEA in hexane); ^{1}H NMR (300 MHz, [D$_6$]benzene, 25 °C): $\delta = 1.18$ (s, 9H; $(CH_3)_3CPh$), 1.39 (m, 1H; C(7)H), 2.08 (m, 1H; C(7)H), 2.41 (s, 1H; C(8)OH), 2.44 (m, 1H; C(4)H), 2.84 (m, 1H; C(4)H), 3.42, 3.45 (2s, 6H; $2CH_3$), 3.89 (m, 1H; C(3)H), 4.21 (d, 1H; $^3J(H,H) = 4.8$ Hz, C(1)H), 4.30–4.42 (m, 1H; one of CH_2CO, 1H; C(6)H, 1H; C(3)H), 4.60 (s, 1H; C(8)H), 4.77 (d, $^3J(H,H) = 7.7$ Hz, 1H; one of CH_2CO), 5.78 (s, 1H; NH), 6.60 (br, 1H; ArH), 6.85 (m, 4H; ArH), 7.14 (m, 1H; ArH), 7.30 (m, 5H; ArH), 7.55 (m, 4H; ArH), 7.71 (d, $^3J(H,H) = 7.4$ Hz, 2H; ArH), 8.12 (d, $^3J(H,H) = 7.0$ Hz, 2H; ArH), 9.89 ppm (s, 1H; NH); ^{13}C NMR (75 MHz, [D$_6$]benzene, 25 °C): $\delta = 31.03$ (q), 32.11 (t), 34.91 (s), 35.07, 53.05 (2t), 54.90, 55.00 (2q), 60.00 (t), 68.09 (s), 77.06, 77.75, 78.45 (3d), 87.09 (s), 113.75, 113.84, 125.81, 127.20, 128.29, 128.92, 131.16, 131.26 (8d), 137.08, 137.38, 146.75, 146.93 (4s), 150.10 (d), 156.23, 159.32, 159.34, 163.69, 167.50 ppm (5s); HRMS, LSI-MS calcd for $C_{45}H_{48}N_4O_8$: 773.3535; found: 773.3536 [M^++H].

Compound 5b: This compound was prepared as described for **5a**, from **4b** (415 mg, 0.49 mmol) and Bu_4NF (296 mg, 0.95 mmol) in THF (3 mL). Compound **5b** (314 mg, 87%) was obtained after flash chromatography (Et_2O/MeOH 9:1 → 8:2) as a white solid. R_f 0.5 (Et_2O/MeOH 8:2); $[\alpha]_D^{25} = +1.32$ ($c = 0.76$ in $CHCl_3$); ^{1}H NMR (300 MHz, [D$_6$]DMSO, 25 °C): $\delta = 0.57$ (d, $^3J(H,H) = 16.6$ Hz, 1H; C(7)H), 1.37 (ddd, $^3J(H,H) = 15.3$, 8.8, 6.4 Hz, 1H; C(7)H), 2.18–2.30 (m, 1H; C(4)H), 2.44–2.49 (m, 1H; C(4)H), 3.61–3.63 (m, 1H; C(1)H, 1H; C(8)H), 3.69–3.75 (m, 6H; CH_3, 1H; C(3)H), 3.88 (dt, $^3J(H,H) = 12.0$, 3.6 Hz, 1H; C(3)H), 4.26 (dd, $^3J(H,H) = 9.4$, 2.8 Hz, 1H; C(6)H), 5.04, 5.11 (2d, $^3J(H,H) = 17.1$ Hz, 2H; CH_2), 5.59 (d, $^3J(H,H) = 2.2$ Hz, 1H; C(8)OH), 6.93–7.00 (m, 4H; ArH), 7.22–7.67 (m, 12H; ArH), 7.85 (s, 1H; NH), 8.04–8.06 (m, 2H; ArH), 8.34, 8.72 (2s, 2H; 2CH), 11.17 ppm (s, 1H; NH); ^{13}C NMR (75 MHz, [D]chloroform, 25 °C): $\delta = 31.58$, 34.34, 45.92 (3t), 55.21 55.23 (2q), 59.54 (t), 67.44 (s), 76.46, 76.98, 77.80 (3d), 86.63 (s), 113.34, 113.38 (2d), 121.94 (s), 127.08, 127.88, 127.99, 128.30, 128.59, 130.54, 132.64 (7d), 133.32, 136.38, 136.61 (3s), 144.04 (d), 145.68, 149.16, 151.70 (3s), 152.23 (d), 158.71, 158.77, 164.93, 165.21 ppm (4s); HRMS, LSI-MS calcd for $C_{42}H_{41}O_7N_6$: 741.3036; found: 741.3037 [M^++H].

Compound 5c: This compound was prepared as described for **5a**, from **4c** (200 mg, 0.24 mmol) and Bu_4NF (150 mg, 0.48 mmol) in THF (1 mL). Compound **5c** (124 mg, 72%) was obtained after flash chromatography (MeOH/CH_2Cl_2 = 1:19 → 1:9) as a white solid. $R_f = 0.50$ (MeOH/CH_2Cl_2 = 1:9, silica gel pre-deactivated by 1% TEA in hexane); ^{1}H NMR (300 MHz, [D]chloroform, 25 °C): $\delta = 1.16$, 1.19 (2d, $^3J(H,H) = 5.49$ Hz, 6H; $2CH_3$), 1.61 (m, 1H; C(7)H), 2.20 (m, 1H; C(7)H), 2.37 (m, 1H; C(4)H), 2.65 (t, 1H; $^3J(H,H) = 6.2$ Hz, C(4)H), 3.10 (m, 1H; CH), 3.75 (s, 6H; $2CH_3$), 3.78–4.09 (m, 2H; C(3)H, 1H; C(6)H, 1H; C(1)H), 4.57 (d, $^3J(H,H) = 7.7$ Hz, 1H; C(8)H), 4.76 (2d, $^3J(H,H) = 22.5$ Hz, 2H; CH_2CO), 6.83 (m, 4H; ArH), 7.15–7.56 (m, 1H; NH, 9H; ArH), 7.63 (s, 1H; CH), 10.19, 12.12 ppm (2s, 2H; NH); ^{13}C NMR (75 MHz, [D]chloroform, 25 °C): $\delta = 18.78$, 19.00 (2q), 32.07, 34.15 (2t), 36.17 (d), 45.99 (t), 55.27, 55.33 (2q), 59.54 (t), 68.01 (s), 74.54, 77.53, 78.75 (3d), 86.34 (s), 113.29, 113.39 (2d), 119.48 (s), 126.90, 127.84, 128.38, 130.39, 130.74 (5d), 136.37, 136.99 (2s), 140.53 (d), 145.83, 147.94, 149.01, 155.77, 158.47, 158.62, 167.38, 179.58 ppm (8s); HRMS, ESI-MS calcd for $C_{39}H_{41}N_6O_8$: 721.2991; found: 721.3002 [M^- − H].

Compound 5d: This compound was prepared as described for **5a**, from **4d** (110 mg, 0.14 mmol) and Bu_4NF (100 mg, 0.32 mmol) in THF (1 mL). Compound **5d** (87 mg, 99%) was obtained after flash chromatography

0947-6539/02/0823-5320 $ 20.00+.50/0 *Chem. Eur. J.* **2002**, *8*, No. 23

(AcOEt) as a white solid. $R_f = 0.22$ (Et_2O/MeOH 9.5:0.5); ^{1}H NMR (400 MHz, [D$_6$]DMSO, 25 °C): $\delta = 0.53$ (d, ^3J(H,H) = 16.2 Hz, 1H; C(7)H), 1.36 (ddd, ^3J(H,H) = 15.7, 9.8, 5.9 Hz, 1H; C(7)H), 1.75 (d, ^4J(H,H) = 1.2 Hz, 3H; CH_3), 2.13 (dt, ^3J(H,H) = 12.6, 7.0 Hz, 1H; C(4)H), 2.42 (dd, ^3J(H,H) = 12.4, 3.1 Hz, 1H; C(4)H), 3.58 (d, ^3J(H,H) < 1 Hz, 1H; C(8)H), 3.61 (d, ^3J(H,H) = 5.7 Hz, 1H; C(1)H), 3.71 (dd, ^3J(H,H) = 11.2, 6.7 Hz, 1H; C(3)H), 3.74 (s, 6H; 2CH_3), 3.84 (dt, ^3J(H,H) = 11.7, 3.4 Hz, 1H; C(3)H), 4.23 (dd, ^3J(H,H) = 9.6, 3.0 Hz, 1H; C(6)H), 4.30, 4.48 (2d, ^3J(H,H) = 16.7 Hz, 2H; CH_2), 5.65 (d, ^3J(H,H) = 2.2 Hz, 1H; C(8)OH), 6.91–6.96 (m, 4H; ArH), 7.20–7.45 (m, 9H; ArH, CH), 7.62 (s, 1H; NH), 11.31 ppm (s, 1H; NH); ^{13}C NMR (75 MHz, [D$_6$]DMSO, 25 °C): $\delta = 12.37$ (q), 32.15, 33.87, 49.74 (3t), 55.54 (q), 59.30 (t), 67.63 (s), 75.79, 77.20, 77.72 (3d), 79.64, 86.14, 108.41 (3s), 113.76, 113.84, 127.20, 128.39, 130.58, 130.70 (6d), 136.71, 136.87 (2s), 142.66 (d), 146.44, 151.50, 158.72, 158.76, 164.79, 168.17 ppm (6s); HRMS (ESI-TOF-MS) calcd for $C_{35}H_{36}N_3O_8$: 626.2502; found: 626.2474 [M^- – H].

Phosphoramidite 6a: Chloro-2-cyanoethyl-diisopropylaminophosphine (0.29 mL, 1.3 mmol) was added at room temperature to a solution of **5a** (335 mg, 0.43 mmol) and *i*Pr$_2$NEt (0.40 mL, 2.3 mmol) in THF (5 mL). After stirring for 3 h under Ar at room temperature, the reaction mixture was quenched with sat. $NaHCO_3$ and extracted (EtOAc). Compound **6a** (378 mg, 88%) was obtained from the organic phase after flash chromatography (AcOEt) as a white foam. $R_f = 0.70$ (AcOEt, silica gel pre-deactivated by 1% TEA in hexane); ^{1}H NMR (300 MHz, [D$_6$]benzene, 25 °C): $\delta = 1.15$, 1.14 (2s, 9H; $(CH_3)_3$CPh), 1.13, 1.11, 1.07, 1.05, 1.03 (5s, 12H; 4CH_3), 1.26–1.34 (m, 1H; C(7)H), 1.58–1.63 (m, 1H; C(7)H), 2.00 (m, 1H; C(4)H), 2.15(m, 2H; CH_2CN), 2.33 (dd, ^3J(H,H) = 12.5, 3.3 Hz, 1H; C(4)H), 3.43, 3.48 (2s, 6H; 2CH_3), 3.19–3.60 (m, 2H; CH_2, 2H; 2CH), 3.76 (m, 1H; C(6)H), 3.89 (m, 1H; C(3)H), 4.20 (d, ^3J(H,H) = 5.5 Hz, 1H; C(1)), 4.36–4.51 (m, 1H; C(3)H, 2H; CH_2CO), 4.70, 4.74 (2s, 1H; C(8)H), 6.17 (s, 1H; NH), 6.89–6.97 (m, 4H; ArH), 7.13–7.32 (m, 3H; ArH), 7.59–7.92 (m, 8H; ArH), 9.07 ppm (s, 1H; NH); ^{13}C NMR (75 MHz, [D$_6$]benzene, 25 °C): $\delta = 20.35$ (t), 24.54, 24.66, 31.99, 30.99 (4q), 34.59 (s), 34.89 (t), 43.25, 43.11, 42.94 (3d), 53.14 (t), 54.90, 54.90, 54.98 (3q), 59.12, 59.34, 60.02 (3t), 66.53, 66.58 (2s), 77.19, 77.35, 78.16 (3d), 87.31 (s), 113.82, 113.97 (2d), 119.02 (s), 125.89, 127.28, 128.35, 128.47, 131.07, 131.24 (6d), 146.80 (s), 149.98 (d), 156.23, 159.41, 159.45, 163.48, 166.43 ppm (5s); ^{31}P NMR (161.9 MHz, [D$_6$]benzene, 25 °C): $\delta = 146.23$, 148.25 ppm; HRMS, ESI-MS calcd for $C_{54}H_{65}N_6O_9P$: 971.4477; found: 971.4462.

Phosphoramidite 6b: This compound was prepared as described for **6a**, from **5b** (340 mg, 0.46 mmol), *i*Pr$_2$NEt (470 μL, 2.54 mmol), and chloro-2-cyanoethyl-diisopropylaminophosphine (300 μL, 1.25 mmol) in THF (5 mL). Compound **6b** (256 mg, 86%) was obtained after extraction (AcOEt/sat. $NaHCO_3$) and chromatography on Sephadex LH 20 as a white foam. $R_f = 0.60$ (AcOEt/MeOH 9:1); ^{1}H NMR (300 MHz, [D]chloroform, 25 °C): $\delta = 0.95$, 0.97, 1.00, 1.02, 1.02, 1.03, 1.05, 1.05 (8s, 12H; 4(CH_3)), 1.41, 1.52 (2d, ^3J(H,H) = 14.5 Hz, 1H; C(7)H), 1.74–1.85 (m, 1H; C(7)H), 2.06, 2.17 (2dd, ^3J(H,H) = 13.2, 3.6 Hz, 1H; C(4)H), 2.49–2.54 (m, 2H; CH_2CN), 2.69–2.72 (m, 1H; C(4)H), 3.29–3.41 (m, 2H; CH_2), 3.53–3.70 (m, 2H; 2CH), 3.80 (s, 6H; CH_3), 3.81–3.86 (m, 1H; C(3)H), 3.95, 4.01 (2d, ^3J(H,H) = 5.2 Hz, 1H; C(1)H), 4.15–4.22 (m, 1H; C(3)H, 1H; C(8)H), 4.35, 4.41 (2d, ^3J(H,H) = 9.9 Hz, 1H; C(6)H), 4.41, 4.55, 4.56, 4.64 (4d, ^3J(H,H) = 15.8 Hz, 2H; CH_2), 5.12, 5.42 (2s, 1H; NH), 6.88–6.94 (m, 4H; ArH), 7.25–7.61 (m, 12H; ArH), 7.99–8.01 (m, 2H; ArH), 8.11, 8.16, 8.71, 8.73 (4s, 2H; 2CH), 9.05, 9.06 ppm (2bs, 1H; NH); ^{13}C NMR (75 MHz, [D]chloroform, 25 °C): $\delta = 20.15$, 20.25, 20.35, 20.43 (4t), 24.19, 24.28, 24.32, 24.38, 24.40, 24.49, 24.51, 24.62 (8q), 30.66, 30.76, 34.05, 34.21 (4t), 42.88, 43.05 (d), 45.68, 46.04 (t), 55.26, 55.29 (q), 57.83, 58.12, 58.16, 58.43, 59.57, 59.76 (6t), 66.04, 66.10 (2s), 76.58, 77.42, 77.48, 77.57 (4d), 86.81, 86.85 (2s), 113.40, 113.46 (2d), 118.06 (s), 127.19, 127.26, 127.78, 128.04, 128.33, 128.79, 130.53, 130.62, 132.64 (9d), 136.10, 136.21, 136.51, 136.56, 143.71, 143.76 (6s), 144.02, 145.00, 145.50, 145.56, 152.46, 158.83, 158.84, 158.87, 158.89, 164.43, 164.82 ppm (11s); ^{31}P NMR (161.9 MHz, [D]chloroform, 25 °C): $\delta = 154.28$, 154.40 ppm; LSI-MS: 942 [M^++H].

Phosphoramidite 6c: This compound was prepared as described for **6a**, from **5c** (126 mg, 0.17 mmol), *i*Pr$_2$NEt (180 μL, 1.1 mmol), and chloro-2-cyanoethyl-diisopropylaminophosphine (115 μL, 0.52 mmol) in THF (1 mL). Compound **6c** (78 mg, 50%) was obtained after flash chromatography (MeOH/EtOAc = 1:9) as a white foam. $R_f = 0.67$ (MeOH/CH_2Cl_2 1:9, silica gel pre-deactivated by 1% TEA in hexane); ^{1}H NMR (300 MHz, [D$_6$]benzene, 25 °C): $\delta = 0.85–1.17$ (m, 12H; 4CH_3, 6H; 2CH_3), 1.23–1.34 (m, 1H; C(7)H), 1.80–2.00 (m, 2H; CH_2CN), 2.32 (t, ^3J(H,H) = 7.0 Hz, 1H; C(7)H), 2.49–2.55 (m, 1H; C(4)H), 2.60–2.83 (m, 1H; C(4)H), 3.08–3.38 (m, 2H; CH_2, 2H; 2CH), 3.50, 3.52, 3.57, 3.59 (4s, 6H; 2CH_3), 3.68 (m, 1H; C(6)H), 3.96 (m, 1H; C(3)H), 4.19 (d, ^3J(H,H) = 5.21 Hz, 1H; C(4)H), 4.40–4.50 (m, 1H; C(3)H), 4.60–4.75 (m, 2H; CH_2CO), 4.91, 5.02 (2s, 1H; C(8)H), 6.33, 6.62 (2s, 1H; NH), 6.96 (m, 4H; ArH), 7.61–7.79 (m, 7H; ArH), 7.97, 8.03 (2s, 1H; CH), 10.14, 12.34 ppm (br, 2H; NH); ^{13}C NMR (75 MHz, [D]chloroform, 25 °C): $\delta = 18.81$, 18.89, 18.94, 19.37 (4q), 20.30, 20.38, 20.45, 20.53 (4t), 24.18, 24.28, 24.38, 24.44, 24.48, 24.55 (6q), 26.86, 29.00, 29.63, 30.79, 31.52, 33.59, 33.93, 34.61 (8t), 36.02, 36.17, 36.22, 41.29, 42.88, 42.98, 43.05, 43.14 (8d), 46.03, 46.25 (2t), 55.30, 55.36 (2q), 58.29, 58.56, 59.67, 59.82 (4t), 66.01, 66.08 (2s), 77.59, 77.73, 77.99, 78.18 (4d), 86.72 (s), 113.38, 113.46 (2d), 118.41, 120.37 (2s), 127.12, 127.21, 127.98, 128.22, 128.29, 130.37, 130.58, 130.76 (8d), 135.99, 136.12, 136.77, 136.86 (4s), 139.39, 139.62 (2d), 145.61, 145.69, 147.66, 148.47, 148.58, 155.48, 155.53, 158.68, 158.80, 158.83, 164.88, 165.28, 178.64, 178.72 ppm (14s); ^{31}P NMR (161.9 MHz, [D$_6$]benzene, 25 °C): $\delta = 148.09$, 149.70 ppm; HRMS, MS-ESI calcd for $C_{48}H_{58}N_8O_9P$: 921.4069; found 921.4048 [M^- – H].

Phosphoramidite 6d: This compound was prepared as described for **6a**, from **5d** (126 mg, 0.17 mmol), *i*Pr$_2$NEt (370 μL, 2 mmol), and chloro-2-cyanoethyl-diisopropylaminophosphine (240 μL, 1 mmol) in THF (2 mL). Compound **6d** (256 mg, 86%) was obtained after flash chromatography (Et_2O/MeOH 9.5:0.5) as a white foam. $R_f = 0.59$ (Et_2O/MeOH 9.5:0.5); ^{1}H NMR (300 MHz, [D]chloroform, 25 °C): $\delta = 1.01$, 1.03, 1.06, 1.08, 1.10 (5s, 12H; 4CH_3), 1.42 (d, ^3J(H,H) = 16.9 Hz, 1H; C(7)H), 1.75–1.86 (m, 1H; C(7)H), 1.88 (s, CH_3), 2.07, 2.15 (2dd, ^3J(H,H) = 12.9, 2.6 Hz, 1H; C(4)H), 2.52–2.61 (m, 2H; CH_2CN), 2.70–2.80 (m, 1H; C(4)H), 3.56–3.48 (m, 2H; CH_2), 3.63–3.71 (m, 2H; 2CH), 3.79 (s, 6H; 2CH_3), 3.82–3.89 (m, 1H; C(3)H), 3.95 (d, ^3J(H,H) = 5.2 Hz, 1H; C(1)H), 3.99 (s, 1H; C(8)H), 4.07–4.18 (m, 2H; CH_2, 1H; C(3)H), 4.35, 4.41 (m, 1H; C(6)H), 4.98, 5.09 (2s, 1H; NH), 6.85–6.90 (m, 4H; ArH), 6.95, 7.04 (2d, ^3J(H,H) < 0.1 Hz, 1H; CH), 7.23–7.48 (m, 9H; ArH), 8.29 ppm (brs, 1H; NH); ^{13}C NMR (100 MHz, [D]chloroform, 25 °C): $\delta = 12.27$ (q), 20.26, 20.32, 20.46, 20.51 (4d), 24.20, 24.27, 24.35, 24.44, 24.49, 24.54, 24.62, 24.70 (8q), 30.75, 30.88 (2t), 34.02, 34.21 (2t), 42.96, 43.08 (2d), 49.22, 49.38 (2t), 55.30 (q), 57.95, 58.17, 58.42, 58.61 (4t), 59.68, 59.81 (2t), 65.84, 65.95 (2s), 77.24, 77.41, 77.49, 77.55 (4d), 86.61, 110.23, 110.33 (3s), 113.39, 113.45 (2d), 118.32 (s), 127.12, 127.22, 128.05, 128.34, 130.57, 130.66 (6d), 136.13, 136.21, 136.48, 136.56 (4s), 140.84, 141.51 (2d), 145.58, 150.54, 150.66, 158.82, 158.86, 163.78, 165.48, 165.80 ppm (7s); ^{31}P NMR (161.9 MHz, [D]chloroform, 25 °C): $\delta = 154.02$, 154.55 ppm; LSI-MS: 828 [M^++H].

Synthesis and purification of the oligonucleotides: All oligonucleotides and analogues were synthesized on the 1.3 μmol scale on a Pharmacia Gene-Assembler Special DNA-synthesizer. Oligodeoxyribonucleotides were synthesized by phosphoramidite chemistry and were assembled, deprotected, and purified according to standard protocols. RNA synthesis was performed with 2′*O*-TBDMS protected phosphoramidites (Glen Research) according to standard protocols for RNA synthesis. Unnatural L-oligoribonucleotides were synthesized with the corresponding 2′*O*-TOM protected L-phosphoramidites as described.[38, 39]

Bicyclo[3.2.1]amide-oligonucleotides were assembled either on CPG-support carrying a natural deoxyribonucleoside unit, or on universal CPG-support from CT-Gen, San José. In the former case, a natural nucleoside remained attached to the 5′-end in a 5′–5′ phosphate linkage, while universal support could tracelessly be removed. Synthesis proceeded with the following changes relative to a DNA synthesis cycle: 1) a 10% trichloroacetic acid solution in dichloroethane was used for detritylation (90 sec), 2) the coupling time was extended to 6 min, and 3) tetrazole (0.45 M in CH_3CN) was replaced by the more active 5-(benzylthio)-1*H*-tetrazole (0.25 M in CH_3CN) as the activator. Coupling yields were typically ≥95%. After removal of the last trityl group, oligonucleotides were detached from the support and deprotected by treatment with conc. NH_3 (55 °C, 17 h for nucleoside modified CPG, 65 °C, 72 h for universal solid support). The crude oligonucleotides were purified by DEAE-HPLC (Mono Q HR 10/10 column, Pharmacia Biotech). Oligonucleotides were desalted over SEP-PAK C-18 cartridges (Waters). All modified oligonucleotides were routinely characterized by ESI$^-$-TOF mass spectrometry (see Table 1).

UV melting experiments and CD spectra: Oligonucleotides were mixed to 1:1 stoichiometry by using the UV extinction coefficients of natural

  0947-6539/02/0823-5321 $ 20.00+.50/0

oligodeoxynucleotides. UV melting curves were recorded on a Cary 3E UV/Vis spectrophotometer (Varian) at 260 nm. Consecutive heating–cooling–heating cycles in the temperature interval of 0–90 °C were applied, with a linear gradient of 0.5 °C min^{-1}. Heating and cooling ramps were superimposable in all cases, indicating equilibrium conditions. CD spectra were measured on a JASCO J-715 spectrometer at the temperatures indicated. Thermodynamic data of duplex formation were determined by the concentration variation method from a plot of T_m^{-1} against ln c, as described.[21]

Molecular modeling: The molecular models of the bicyclo[3.2.1]amide nucleic acid duplexes were built with the molecular modeling program suite Moloc.[40, 41] In particular, the highly resolved A-RNA homopurine/homopyrimidine duplex (X-ray structure of $r^D(G_{11})\cdot r^D(C_{11})$ determined at 1.20 Å,[42] protein database code 1QCU) served as starting geometry. The phosphate backbone was rendered neutral by uniform hydrogen saturation. The structure was subsequently subjected to energy optimization within the force field MAB,[43] which generally leads to a flattening out and regularization within the base-pair planes, whereafter the latter were changed into adenine and thymine residues and reoptimized, first with fixed backbone geometry, then by releasing the whole structure. This "idealized" $r^D(A_{11})\cdot r^D(T_{11})$ duplex was then transformed into $r^D(A_{10})\cdot r^D(T_{10})$ and mirrored into $r^L(A_{10})\cdot r^L(T_{10})$, and the energies of both were reoptimized to form the prototypes for further transformations. In particular, 10-mer homoadenine and homothymine strand constitutions of bicyclo[3.2.1]amide nucleic acid were superimposed onto both the left-handed and the right-handed duplex templates by use of a flexible optimization match algorithm contained in the modeling suite. The backbones were substituted and fused to the template base-pairs, which were kept fixed in the first optimization cycles to establish standard bond lengths at the attachment points. The backbone was then regularized with weak hydrogen-bond constraints applied between intrastrand amide groups: through this procedure the *endo*[3.2] amide group conformation was identified to allow significant left-handed base-pair "staircase" overlap, whereas the *endo*[3.1] amide conformer was found to fit with right-handed base-pair overlap (Figure 8). The *endo*[2.1] amide rotamer does not lead to any hydrogen-bond-like inter-residual β-turn, and was thus rejected for inclusion in the right- and left-handed oligomer structures; moreover, according to isolated energy terms, the *endo*[2.1] rotamer is intrinsically disfavored by slightly more than 1 kcal mol^{-1} (Figure 7). After regularization of the modified backbone geometries, all constraints were removed and the duplexes were completely relaxed in the force field.

Acknowledgement

The authors thank the Swiss National Science Foundation (grant No. 20–63582.00) and Novartis AG, Basel, for continuing financial support.

[1] S. M. Freier, K.-H. Altmann, *Nucleic Acids Res.* **1997**, *25*, 4429–4443.
[2] J. Hunziker, H.-J. Roth, M. Böhringer, A. Giger, U. Diederichsen, M. Göbel, R. Krishnan, B. Jaun, C. Leumann, A. Eschenmoser, *Helv. Chim. Acta* **1993**, *76*, 259–352.
[3] C. Hendrix, H. Rosemeyer, I. Verheggen, F. Seela, A. Van Aerschot, P. Herdewijn, *Chem. Eur. J.* **1997**, *3*, 110–120.
[4] J. Wang, B. Verbeure, I. Luyten, E. Lescrinier, M. Froeyen, C. Hendrix, H. Rosemeyer, F. Seela, A. Van Aerschot, P. Herdewijn, *J. Am. Chem. Soc.* **2000**, *122*, 8595–8602.
[5] Y. Maurinsh, H. Rosemeyer, R. Esnouf, A. Medvedovici, J. Wang, G. Ceulemans, E. Lescrinier, C. Hendrix, R. Busson, P. Sandra, F. Seela, A. Van Aerschot, P. Herdewijn, *Chem. Eur. J.* **1999**, *5*, 2139–2150.
[6] S. Pitsch, S. Wendeborn, B. Jaun, A. Eschenmoser, *Helv. Chim. Acta* **1993**, *76*, 2161–2183.
[7] S. Honzawa, S. Ohwada, Y. Morishita, K. Sato, N. Katagiri, M. Yamaguchi, *Tetrahedron* **2000**, *56*, 2615–2627.
[8] J.-M. Henlin, K. Jaeckel, P. Moser, H. Rink, E. Spieser, G. Baschang, *Angew. Chem.* **1992**, *104*, 492–493; *Angew. Chem. Int. Ed. Engl.* **1992**, *31*, 482–483.
[9] P. Nielsen, F. Kirpekar, J. Wengel, *Nucleic Acids Res.* **1994**, *22*, 703–710.
[10] L. Peng, H.-J. Roth, *Helv. Chim. Acta* **1997**, *80*, 1494–1512.
[11] K. C. Schneider, S. A. Benner, *J. Am. Chem. Soc.* **1990**, *112*, 453–455.
[12] K. Schoning, P. Scholz, S. Guntha, X. Wu, R. Krishnamurthy, A. Eschenmoser, *Science* **2000**, *290*, 1347–1351.
[13] C. J. Leumann, *Bioorg. Med. Chem.* **2002**, *10*, 841–854.
[14] C. Epple, C. Leumann, *Chem. Biol.* **1998**, *5*, 209–216.
[15] C. D. Roberts, C. Epple, C. J. Leumann, *Nucleosides Nucleotides* **1999**, *18*, 1413–1415.
[16] B. M. Keller, C. J. Leumann, *Angew. Chem.* **2000**, *112*, 2367–2369; *Angew. Chem. Int. Ed.* **2000**, *39*, 2278–2281.
[17] A. Egger, J. Hunziker, G. Rihs, C. Leumann, *Helv. Chim. Acta* **1998**, *81*, 734–743.
[18] Z. Timár, L. Kovács, G. Kovács, Z. Schmél, *J. Chem. Soc. Perkin 1* **2000**, 19–26.
[19] D. W. Will, G. Breipohl, D. Langner, J. Knolle, E. Uhlmann, *Tetrahedron* **1995**, *51*, 12069–12082.
[20] K. L. Dueholm, M. Egholm, C. Behrens, L. Christensen, H. F. Hansen, T. Vulpius, K. H. Petersen, R. H. Berg, P. E. Nielsen, O. Buchardt, *J. Org. Chem.* **1994**, *59*, 5767–5773.
[21] L. A. Marky, K. J. Breslauer, *Biopolymers* **1987**, *26*, 1601–1620.
[22] A. Egger, C. J. Leumann, *Synlett* **1999**, *S1* 913–916.
[23] M. Marangoni, A. Van Aerschot, P. Augustyns, J. Rozenski, P. Herdewijn, *Nucleic Acids Res.* **1997**, *25*, 3034–3041.
[24] S. Fujimori, K. Shudo, Y. Hashimoto, *J. Am. Chem. Soc.* **1990**, *112*, 7436–7438.
[25] A. Garbesi, M. L. Capobianco, F. P. Colonna, L. Tondelli, F. Arcamone, G. Manzini, C. W. Hilbers, J. M. E. Aelen, M. J. J. Blommers, *Nucleic Acids Res.* **1993**, *21*, 4159–4165.
[26] V. K. Rajwanshi, A. E. Hakansson, M. D. Sorensen, S. Pitsch, S. K. Singh, R. Kumar, P. Nielsen, J. Wengel, *Angew. Chem.* **2000**, *112*, 1722–1725; *Angew. Chem. Int. Ed.* **2000**, *39*, 1656–1659.
[27] R. Krishnamurthy, S. Pitsch, M. Minton, C. Miculka, N. Windhab, A. Eschenmoser, *Angew. Chem.* **1996**, *108*, 1619–1623; *Angew. Chem. Int. Ed. Engl.* **1996**, *35*, 1537–1541.
[28] S. Pitsch, R. Krishnamurthy, M. Bolli, S. Wendeborn, A. Holzner, M. Minton, C. Lesueur, I. Schönvogt, B. Jaun, A. Eschenmoser, *Helv. Chim. Acta* **1995**, *78*, 1621–1635.
[29] M. Egholm, O. Buchardt, L. Christensen, C. Behrens, S. M. Freier, D. A. Driver, R. H. Berg, S. K. Kim, B. Norden, P. E. Nielsen, *Nature* **1993**, *365*, 566–568.
[30] E. Uhlmann, A. Peyman, G. Breipohl, D. W. Will, *Angew. Chem.* **1998**, *110*, 2954–2983; *Angew. Chem. Int. Ed.* **1998**, *37*, 2796–2823.
[31] B. Hyrup, P. E. Nielsen, *Bioorg. Med. Chem.* **1996**, *4*, 5–23.
[32] Ö. Almarsson, T. C. Bruice, *Proc. Natl. Acad. Sci. USA* **1993**, *90*, 9542–9546.
[33] Ö. Almarsson, T. C. Bruice, J. Kerr, R. N. Zuckermann, *Proc. Natl. Acad. Sci. USA* **1993**, *90*, 7518–7522.
[34] S. C. Brown, S. A. Thomson, J. M. Veal, D. G. Davis, *Science* **1994**, *265*, 777–780.
[35] L. Betts, J. A. Josey, J. M. Veal, S. R. Jordan, *Science* **1995**, *270*, 1838–1841.
[36] M. Koga, S. W. Schneller, *Nucleic Acids Symp. Ser.* **1993**, *29*, 63–65.
[37] M. Tarköy, M. Bolli, C. Leumann, *Helv. Chim. Acta* **1994**, *77*, 716–744.
[38] S. Pitsch, *Helv. Chim. Acta* **1997**, *80*, 2286–2314.
[39] S. Pitsch, P. A. Weiss, L. Jenny, A. Stutz, X. Wu, *Helv. Chim. Acta* **2001**, *84*, 3773–3795.
[40] P. R. Gerber, Moloc—A Molecular Design Software Suite (http://www.moloc.ch).
[41] C. Lehmann, *Chimia* **2000**, *54*, 469.
[42] C. Klosterman, S. A. Shah, T. A. Steitz, *Biochemistry* **1999**, *38*, 14784–14792.
[43] P. R. Gerber, K. Müller, *J. Comput.-Aided Mol. Des.* **1995**, *9*, 251–268.

Received: June 6, 2002 [F4163]

